Geomorphology 277 (2017) 17–30

Contents lists available at ScienceDirect

Geomorphology

journal homepage: www.elsevier.com/locate/geomorph

Sediment pulse evolution and the role of network structure

Karen B. Gran [a,c], Jonathan A. Czuba [b,c]

[a] Department of Earth & Environmental Sciences, University of Minnesota Duluth, Duluth, MN, USA
[b] Department of Civil, Environmental, and Geo-Engineering, St. Anthony Falls Laboratory, University of Minnesota, Minneapolis, MN, USA
[c] National Center for Earth-surface Dynamics, University of Minnesota, Minneapolis, MN, USA

ARTICLE INFO

Article history:
Received 3 September 2015
Received in revised form 9 December 2015
Accepted 18 December 2015
Available online 21 December 2015

Keywords:
Sediment wave
Sediment pulse
Network routing
Sediment connectivity

ABSTRACT

Sediment pulses are triggered through a variety of mechanisms, from landslides to land use change. How do these pulses move through the fluvial system, and how do they evolve? In a system with perfect sediment connectivity, the erosional response to a perturbation and the resulting signal at the river mouth would match, however, this rarely occurs. Many studies have addressed reach-scale dynamics of sediment pulses and how they translate or disperse downstream. At the watershed scale, network structure and storage become more important in modulating the sediment signal. Here, we review the current literature on sediment pulse behavior, and then address the role of network structure on maintaining, dispersing, or transforming sediment pulses in a fluvial system. We use a reduced-complexity network routing model that simulates the movement of bed material through a river basin. This model is run in the Greater Blue Earth River (GBER) basin in Minnesota, USA, first with spatially uniform inputs and then with inputs constrained by a detailed sediment budget. Once the system reaches equilibrium, a sediment pulse is introduced, first at a single location and then throughout the system, and tracked as it evolves downstream. Results indicate that pulses able to translate downstream disperse in place upon arriving at over-capacity reaches as sediment goes into storage. In the GBER basin, these zones occur just upstream of a knickpoint that is propagating upstream through all mainstem channels. As the pulses get caught in these sediment "bottlenecks," there is a decoupling of the original pulse of sediment and the resulting bed material wave. These results show that the network structure, both in terms of network geometry and the spatial pattern of transport capacity, can play a dominant role in sediment connectivity and should be considered when predicting sediment pulse behavior at the watershed scale.

1. Introduction

How well is the integrity of an erosional signal preserved and maintained during transport downstream? In a system with perfect sediment connectivity, the signal at the outlet would mimic the erosional signal upstream with an associated time lag. If there was perfect connectivity between the erosional response to a perturbation (say, climate change), and the sedimentary deposit left behind, then one could "read the rocks" and back-out the erosional history of the basin. Fundamentally, it is the fluvial system that propagates an erosional signal from the uplands to a depositional basin. How that signal is transmitted depends upon the nature of the perturbation including magnitude, frequency, duration, and spatial extent; the distance from source to sink; and characteristics of the fluvial system and sediment transport processes within it, including storage effects.

This paper focuses on perturbations that deliver excess sediment to fluvial systems and how well those signals are preserved from upstream source to river outlet. Perturbations that produce excess sediment above background rates vary from single high-magnitude inputs to longer-term shifts in total sediment yield. Here, we discuss a range of sediment inputs in fluvial systems and how they evolve as they propagate downstream through a review of field cases and numerical and physical modeling efforts. We first review research on the evolution of sediment waves from single pulses of sediment (i.e. from landslide, dam removal, or volcanic inputs) to persistent or widespread disturbances (i.e. from widespread land use or climate change). There have been many studies on reach-scale sediment wave dynamics in the literature (i.e. Meade, 1985; Nicholas et al., 1995; Lisle et al., 1997, 2001; Sutherland et al., 2002; Cui et al., 2003a, 2003b, 2005; Lisle, 2008; Sklar et al., 2009; Venditti et al., 2010a; Humphries et al., 2012; Nelson et al., 2015). At the watershed scale, however, tributary interactions and storage may occur, leading to potential synchronizations and additional transformations of the original sediment wave (Jacobson, 1995; Benda and Dunne, 1997a, 1997b; Jacobson and Gran, 1999; Benda et al., 2004a; James, 2010; Czuba and Foufoula-Georgiou, 2014, 2015), increasing the complexity of downstream transport.

To help bridge the gap from reach-scale dynamics to watershed-scale sediment connectivity, a reduced-complexity network routing model developed by Czuba and Foufoula-Georgiou (2014, 2015) is used to study how network structure and storage may affect the potential for creation, persistence, or dispersion of sediment waves. Here, network structure refers to both the geometry of tributary inputs as

http://dx.doi.org/10.1016/j.geomorph.2015.12.015

well as the spatial pattern of transport capacity. The model is run in a well-studied basin in southern Minnesota, USA, to enable realistic sediment inputs for comparison with more spatially-uniform inputs, and track how sediment pulses evolve as they move downstream through the watershed. To assess the role of network structure vs. spatial pattern of inputs on the sediment signal downstream, a run with spatially uniform sediment inputs is compared to one with inputs constrained by a detailed sediment budget. The model is then set up to allow in-channel storage and run to investigate how different aspects of network structure, including both network geometry and the spatial pattern of transport capacity affect the downstream propagation of sediment pulses.

2. Background

Sediment is supplied to the fluvial network primarily through overland flow, mass movements, and fluvial scour. Hillslope erosion may transport sediment slowly and steadily into channels through processes like creep, or sediment may be stored in colluvial hollows or fans and released episodically via landslides or debris flows. Inputs from bank scour and bluff collapse through mass wasting occur preferentially during high flow events, leading to stochastic inputs directly to the stream. Perturbations to the watershed, including seismic activity, heavy rainfall events, forest fires, or land use changes can increase the volume of sediment supplied to a stream network from both colluvial and near-channel sources. On one end of the spectrum are single inputs of excess sediment, isolated in time and space from, for example, landslides or dam removals. On the other end are spatially-extensive pervasive sediment perturbations, for example from land use conversion to agriculture. In this case, much of the watershed may be disturbed, and in some cases the change in sediment input to the channel may be more of a step function rather than a single pulse. In between are a range of other input characteristics, from single-pulse widespread sediment perturbations, perhaps from a wildfire, to long-term point source inputs from mining operations.

There have been many studies on sediment wave dynamics in the literature, with much of the recent research focused specifically on reach-scale sediment waves and how a single point source input evolves through time. Fewer studies have looked at sediment wave propagation at the watershed scale, where potential synchronizations in the landscape may affect how sediment pulses move downstream, what the resulting depositional signal might look like, and how channels will respond to management options designed to lower sediment inputs. Here, we review studies from the field, flume, and numerical modeling for different end members of sediment input. Two recent review papers cover reach-scale sediment pulse evolution (Lisle, 2008) and watershed-scale high-magnitude sediment wave evolution (James, 2010). We review and update those findings and then examine some of the elements that link reach-scale transport with watershed-scale sediment signals, including network structure and the effects of storage, elements that are then investigated further through a watershed-scale network routing and transport model.

2.1. Nomenclature

Gilbert (1917) was one of the first to report on sediment waves in watersheds, noting the downstream migration of hydraulic mining debris from the Sierra Nevada across the central valley of California. He used the term "sediment wave" to describe the wavelike movement of sediment as it transported downstream. The wavelike behavior was most notable in the rise and fall of channel bed elevations due to passage of the excess mining debris. Later studies by James (1989, 1991, 1993) showed that the passage of sediment was much more complex. Due to temporary storage of excess sediment in the floodplain, high sediment loads persisted much longer than the initial bed wave which has led some to prefer alternate terminologies. Nicholas et al. (1995) prefer the more generic term sediment "slug" to include excess sediment that does not conform to wavelike behavior, although Lisle (2008) notes that the term "slug" does not properly address sediment mobilized that was not part of the initial sediment input. The term slug was further refined to reflect the magnitude of the inputs (macroslug, megaslug, and superslug) and thus the spatial scale of impact, from minor channel impacts at the scale of gravel bars up to major valley-floor adjustments spanning kilometers of channel or more (Nicholas et al., 1995).

Another commonly used term to refer to excess sediment inputs is sediment "pulse". Traditionally, the term sediment pulse referred to zones with high sediment transport rates (Reid et al., 1985; Iseya and Ikeda, 1987), but more recently the term has been used to refer to discrete sediment inputs (Cui et al., 2003a). Cui et al. (2003a, 2003b) prefer the term "pulse" over "wave" or "slug" noting that not all sediment pulses exhibit wavelike behavior. Later papers by the same authors use the term sediment "pulse" and sediment "wave" interchangeably (Cui and Parker, 2005; Cui et al., 2005). Here, we opt for that approach and use the term sediment pulse and sediment wave interchangeably to describe the influx and movement of a volume of excess sediment in a fluvial system.

2.2. Reach-scale sediment pulses

First consider a pulse of sediment entering a channel at a discrete point in space and time, perhaps from a landslide or debris flow or generated through a dam removal (e.g. Hansler, 1999; Sutherland et al., 2002; Major et al., 2012; East et al., 2015). Sediment pulses can both disperse and translate downstream. As the pulse evolves, sediment can move into longer-term storage on the floodplain or be permanently lost due to comminution. Research into reach-scale pulse dynamics initially focused on documenting sediment wave passage in the field (Gilbert, 1917; Pickup et al., 1983; Meade, 1985; James, 1989; Knighton, 1989, 1991; Madej and Ozaki, 1996; Sutherland et al., 2002) and over time has shifted more towards targeted experiments and model development (Lisle et al., 2001; Cui et al., 2003a, 2003b, 2005; Cui, 2007; Sklar et al., 2009; Venditti et al., 2010a; Humphries et al., 2012) to understand how sediment pulses evolve and to develop a more detailed understanding of which conditions favor dispersion vs. translation.

Initially, it was assumed that sediment waves translated downstream based on a series of field observations, starting with the early work of Gilbert (1917) and the California hydraulic mining debris. Although this particular field case is of a much greater magnitude than most point-source inputs, it had a dominant effect on how people thought about sediment wave migration. The main set of observations made by Gilbert (1917) indicating a wave-like passage of sediment were bed elevations that went up as the hydraulic mining debris arrived and then later went down after passage of the wave of sediment. Later studies by Knighton (1989, 1991) in Tasmania also documented the wave-like progression of mining debris downstream, recorded by the rise and fall of gages along the channel over the course of decades. In both cases, however, there are confounding factors. First, a significant volume of sediment moved into storage in the floodplain as the sediment wave propagated downstream, complicating interpretations of the timescales of adjustment. Second, one of the main observations, that gage elevations went up and then down as the wave passed, is not necessarily an indication of wave translation. The passage of a wave of sediment looks remarkably similar to dispersion in place of the same sediment as viewed through gage elevations, as dispersion also leads to rise and subsequent fall of downstream gages (see Fig. 1). The difference lies in the magnitude of the bed elevation response and in the behavior of the mass of sediment overall. For a sediment wave to be purely translational, the head, tail, and center of mass of the sediment wave must all move downstream at the same pace.

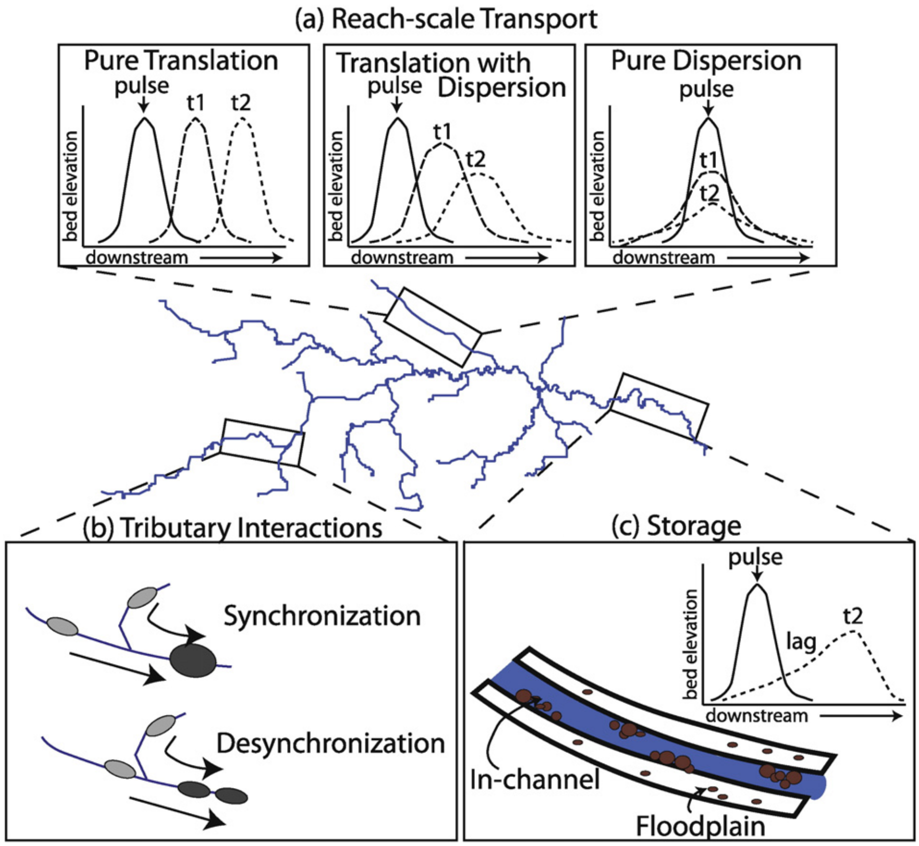

Fig. 1. Conceptual figure showing potential influences on sediment pulse movement in a watershed including (a) reach-scale dynamics that lead to either dispersion, translation, or a combination of both; (b) tributary interactions that can both synchronize or desynchronize sediment waves moving downstream, and (c) in-channel and floodplain storage that leads to a lag in the sediment wave movement downstream.

Several field studies have noted the asymmetrical passage of a sediment wave, with a long tail to the distribution attributed to sediment storage and release over time (Pickup et al., 1983; James, 1989, 1991, 1993; Madej and Ozaki, 1996). Pickup et al. (1983) studied the downstream migration of mining sediment in the Kawerong River in Papua New Guinea and found that in order to model the downstream migration of the sediment wave accurately, a significant element of dispersion had to be included. The “translational” mining debris cases reviewed above all saw the amplitude of the bed elevation wave decrease with distance downstream, which could be interpreted as a sign of dispersion, not translation of the sediment wave. Sediment input from the Navarro landslide in California was well-documented enough to determine that essentially no translation occurred, and the sediment pulse associated with the slide dispersed in place (Hansler, 1999; Lisle et al., 2001; Sutherland et al., 2002).

The conundrum of sediment wave behavior (translation vs. dispersion) began to receive significant attention in the late 1990s and early 2000s. This included an important series of experiments by Lisle et al. (1997, 2001) on sediment wave propagation. Lisle et al. specifically looked at single inputs of sediment at a reach-scale, with no floodplain storage or network-scale effects. The sediment pulses were of a significant enough magnitude to affect the local hydraulics. Several parameters were varied including the grain size distribution of both the sediment pulse and bed surface. They found that in all cases considered, the sediment pulse largely dispersed in place. A significant component of translation was only seen in the fine-grained (sand) pulse over a gravel-bed.

Numerical modeling of single pulse inputs of sediment have focused primarily on pulses that are significant enough to perturb the flow field (Lisle et al., 2001; Cui and Parker, 2005; Cui et al., 2006). Backwater effects upstream of the pulse lead to deposition, while increased slopes on the downstream side of the pulse lead to higher transport rates. As summarized in Lisle (2008), all of the model solutions for 1D steady flow indicate the dominance of dispersion except in cases of low Froude number flows and sediment inputs that are finer than bed sediment (Lisle et al., 1997; Cui and Parker, 2005). Since typical gravel-bed rivers transport sediment under high Froude number conditions, one might expect most sediment pulses in gravel-bed channels to disperse in place, with translation more likely in sand-bedded channels. These findings mirror field cases in which elements of translation were apparent primarily in low Froude number flows where sand waves were found moving over gravel or cohesive clay beds (Meade, 1985; Wohl and Cenderelli, 2000; Bartley and Rutherfurd, 2005).

Later flume studies found similar trends to numerical model results, with significant pulse translation only occurring in flows with low Froude numbers and dispersion dominating in high Froude number flows (Cui et al., 2003a, 2003b), but as additional data are collected, a more complex understanding of pulse behavior arises. Pulses with a large magnitude of sediment relative to the channel load such that the flow field is actually perturbed lead to more dispersive behavior than small sediment pulses that do not strongly perturb the flow field (Sklar et al., 2009). Further flume studies on grain size effects reinforce the earlier observation that finer-grained sediment travelling over a coarser-grained bed can translate more than disperse (Cui et al., 2003a; Sklar et al., 2009), particularly when there is no sediment being fed from upstream (Sklar et al., 2009; Humphries et al., 2012). Sediment inputs that are substantially finer than the bed surface can also mobilize extra material from the bed, further increasing downstream transport rates (Venditti et al., 2010a, 2010b). The increase in transport rates associated with overall bed fining helps explain the rapid translation of fine-grained mining debris out of the upper Fraser River in British Columbia (Ferguson et al., 2015). There, it was the ratio of the fine-grained gravel inputs to the coarser-grained bed that was important, as opposed to sand specifically overlying gravel, a distinction also noted in flume experiments by Venditti et al. (2010b).

One of the challenges of interpreting sediment pulse behavior is that channels respond in many ways to sediment pulses beyond simple cycles of aggradation and incision, and recovery from the passage of a sediment wave can involve more than just return to a pre-disturbance bed elevation. In cases where the grain size of the excess sediment is finer than the bed material, the main response to passage of a sediment wave may be a fining of the bed and increase in bedload transport rates as the channel evolves to accommodate an increased sediment load, with recovery signified by a coarsening of bed texture and/or a reduction in transport rates (Gran and Montgomery, 2005; Sklar et al., 2009; Venditti et al., 2010a, 2010b; Gran, 2012; Ferguson et al., 2015). Additional variables that can change with increased sediment inputs include channel complexity, pool abundance and capacity, sediment thickness, and degree of bedrock exposure (Wohl and Cenderelli, 2000; Kasai et al., 2004; Bartley and Rutherfurd, 2005; Hoffman and Gabet, 2007; East et al., 2015), with passage of the sediment wave noted by a return to pre-disturbance complexity.

More recently, dam removals have provided opportunities to study large single-pulse inputs to a natural stream channel, but in a more controlled environment (i.e. Major et al., 2012; Tullos and Wang, 2014; Wilcox et al., 2014; East et al., 2015). These studies generally have the simplicity of a well-timed release of sediment from a single point source, often with well-documented conditions before, during, and after the sediment release. They vary in terms of the rate of drawdown and release of water, volume of sediment removed at the time of the dam breach, and grain size impounded behind the dam as well as site-specific channel and flow conditions. In most cases, downstream aggradation was noted, first in the main channel and then, if available, in floodplain channels. Aggradation was followed by incision, leaving deposits in the floodplain or as new bars in the system. The timescale for bed adjustment varied widely depending on both the rate of dam breach and the grain size of sediments impounded behind the dam. Channels below dams with rapidly-released, fine-grained sediments were more able to adjust rapidly and recover from the sediment release associated with the dam breach than channels where the breach occurred over a longer time period or where reservoir sediments were less easily mobilized (Major et al., 2012; Tullos and Wang, 2014; Wilcox et al., 2014; East et al., 2015).

2.3. Role of storage

Many of the sediment pulses introduced by dam removals referenced above were large enough to cause a significant fraction of the material to go into transient storage within the channel or longer-term storage in the floodplain. For high-magnitude pulses like these, storage can play a dominant role on the overall evolution of the sediment pulse.

Within the channel corridor itself, sediment can be stored on point bars or behind large wood jams. In-channel storage does not stay constant or monotonically increase downstream, but can be distributed into discrete “disturbance” or “sedimentation” zones interspersed with more stable reaches that lack significant in-channel storage (Church, 1983; Saucier, 1983; Macklin and Lewin, 1989; Jacobson, 1995; Benda et al., 2004a, 2004b). Disturbance zones may be characterized by higher lateral migration rates, leading to greater rates of floodplain exchange with active channels, than reaches with less in-channel storage. In some cases, sedimentation reaches are related to network configuration and are found at tributary junctions (Church, 1983; Rice, 1998; Benda et al., 2004a; Ferguson et al., 2006), while in other cases, they may be related more to valley-channel interactions or bedrock controls (Magilligan, 1985; Macklin and Lewin, 1989). These reach-scale complexities can lead to a pattern where sediment moves from one sedimentation zone to the next. Pulse dispersion can be enhanced due to sediment loss to and slow release from storage zones, or pulse integrity can be maintained as sediment collects in each disturbance reach and then moves downstream to the next one (Meade, 1985; Jacobson and Gran, 1999).

Many of the flume experiments and 1D models cited above lack in-channel complexity at a reach-scale and network-scale complexities at watershed scales. Floodplain storage is specifically avoided in many experiments and models in order to focus on in-channel evolution of the sediment pulse. Several recent flume experiments have begun to incorporate in-channel complexity to investigate the role of alternate bar sequences (Humphries et al., 2012) and variable channel width (Nelson et al., 2015) on sediment pulse evolution. Nelson et al. (2015) found that the pool-riffle structure set up by varying channel width enhanced dispersion suggesting that the in-channel complexity found in natural systems may play an important role in sediment wave evolution. Both Hassan et al. (2005) and Kasai et al. (2004) noted that in-channel complexity and storage can play a critical but complex role in the behavior of sediment pulses moving through fluvial systems. In small, mountainous channels, sediment stored in the channel can be as much as ten times the annual sediment yield. Sediment released from these in-channel storage elements can generate internal sediment pulses in the system, while storage of externally-generated sediment pulses in these storage areas can act to attenuate sediment waves (Hassan et al., 2005).

In addition to in-channel storage, high-magnitude sediment pulses can deposit sediment into longer-term storage in the floodplain. Sediment pulses that lead to substantial floodplain storage were reviewed by James (2010). He notes that sediment inputs can lead to aggradation-degradation events with substantial sediment moving into storage in the floodplain during the aggradation phase. During the degradation phase, even though the river bed may return to its pre-disturbance elevation, sediment stored in the floodplains and slowly released back to the channel through lateral migration lengthens the timescale for recovery over what would be predicted based on bed elevations alone. Elevated sediment transport rates may persist much longer than bed elevation adjustments, causing a disconnect between the channel bed wave and the sediment wave itself (James, 2010). The sediment wave incorporates sediment that moves into and later out of floodplain storage, and thus persists for much longer than the channel bed wave (Macklin and Lewin, 1989; James, 2010). In this sense, the sediment wave is not a typical wave-form moving through the channel as a coherent unit, but rather a drawn-out period with higher near-channel sediment inputs, transport rates, and/or altered in-channel geomorphology.

2.4. Watershed-scale sediment pulses

Sediment can be input into a stream not just at a single point, but throughout the watershed. This can occur naturally due to widespread landsliding following a seismic event or wildfire, high-magnitude rainfall event, or volcanic eruption (Pearce and Watson, 1986; Keefer, 1994; Benda et al., 2003; Dadson et al., 2004; Gran and Montgomery, 2005; Hoffman and Gabet, 2007; Tullos and Wang, 2014). Anthropogenic alterations to the landscape can also lead to substantial widespread sediment inputs, for example from mining (Gilbert, 1917; Lewin et al., 1983; Pickup et al., 1983; Knighton, 1989, 1991; James, 1989, 1991, 1993, 2010) or land clearing for agriculture, grazing, or forestry (Trimble, 1981, 1983, 1994; Reid and Dunne, 1984; Jacobson, 1995; Jacobson and Primm, 1997; Fitzpatrick et al., 1999; Jacobson et al., 2001; Belmont et al., 2011; Gran et al., 2013). As soon as the spatial scale grows beyond a single pulse in a single reach, channel network structure must be considered.

Network structure dictates how inputs from diffuse sources interact at tributary junctions, either dispersing or enhancing sediment pulses moving downstream (Fig. 1). This can include both the spatial arrangement of tributary junctions as well as the spatial pattern of transport capacity, a function of basin size, slope, and channel width. Benda and

Dunne (1997a, 1997b) recognized that sediment waves moving downstream are transformed not just by translation, dispersion, and abrasion, but also by "mutual interference at tributary junctions", a topic explored further by Benda et al. (2004a, 2004b). Jacobson and Gran (1999) developed a simple routing model for gravel in Ozark streams and found that widely-dispersed gravel inputs from land use changes that moved steadily through the channel network could accumulate into a series of sediment waves moving through the mainstem channel; in this case the waveform was enhanced by positive interference at tributary junctions rather than dispersed due to storage. Likewise, Czuba and Foufoula-Georgiou (2014, 2015) found that sediment sourced from different tributary valleys in different events could lead to larger sediment waves in the mainstem channel depending on the timing of events and the compounding effects of network structure. Jacobson (1995) noted that the shape and pattern of the drainage network affected how sediment waves developed and moved through the system, with dendritic networks leading to more positive interference at tributaries and wave-like bed elevation changes at downstream gages. Basin shape affects the likelihood that contributing tributaries will have a drainage area large enough to have a geomorphic effect on mainstem channels (Benda et al., 2004a). Ferguson et al. (2006) quantified these relationships, showing that the ratio of discharge flux, sediment flux, and bedload diameter between the mainstem channel and an entering tributary are all important in determining the impact tributaries can have on mainstem sediment transport. Abundant tributary inputs and tributary inputs with unique grain size distributions compared to the mainstem have the biggest geomorphic impact on mainstem channels (Rice, 1998). Specific configurations of channels, for instance where several geomorphically-significant tributaries enter the mainstem channel in close proximity, can be hotspots of geomorphic change (Benda et al., 2004a).

Czuba and Foufoula-Georgiou (2014) developed a reduced-complexity network routing model to track sediment that was input at a single instant in time uniformly throughout all channels in the watershed, tracking the "sedimentograph" produced for different grain sizes. The results mimic those of Jacobson and Gran (1999) in that a single widespread pulse developed into a series of sediment waves at the mouth of the river. Czuba and Foufoula-Georgiou (2015) also noted distinct zones with higher sediment persistence, essentially places where sediment accumulates in the network due to the interplay between network structure and local channel characteristics. Several of these areas correlate strongly with high rates of historic channel migration (Bevis, 2015; Czuba and Foufoula-Georgiou, 2015). When these reaches remain below capacity, sediment is able to move through them readily and the signal observed at the mouth of the channel is fundamentally driven by network geometry alone. When sediment loading increases, however, these zones of high sediment persistence may become storage zones, attenuating and lengthening the sediment signal coming out of the basin. Thus, the network structure may affect reach-scale change differently under conditions of low vs. high sediment supply, and the spatial organization of reaches above and below capacity dictates how a pulse moves through the network. This is an aspect of sediment connectivity and pulse evolution that has not been well-explored.

3. Methods

Given that many elements in the fluvial system tend to disperse sediment waves, from reach-scale pulse evolution to dispersion associated with storage, network interactions seem to be one of the few processes that can actually maintain or even enhance wave-like behavior. From a sediment connectivity standpoint, both network geometry and the spatial patterns of transport capacity play an integral role in maintaining, dispersing, or transforming sediment pulses in a fluvial system. To further address the role of network structure on sediment wave evolution, a reduced-complexity network routing model developed by Czuba and Foufoula-Georgiou (2014, 2015) is used that simulates the movement of water and sediment through a river basin. This work is motivated in part by earlier sediment routing models by Benda and Dunne (1997a, 1997b) that simulated the stochastic supply and downstream transport and modification of sediment in a mountainous environment where sediment supply was dominated by mass wasting and sediment travels as gravel-rich bedload. The landscape used for the model presented here has most of the sediment supplied in downstream reaches, and significant anthropogenic influences and changes in hydrology over the last two centuries have driven an order of magnitude increase in sediment supply (Engstrom et al., 2009; Belmont et al., 2011; Schottler et al., 2013).

The model of Czuba and Foufoula-Georgiou was used to explore different ways sediment pulses may be modified at the watershed scale as they transport downstream. Initial runs with spatially-uniform sediment inputs indicate that the network develops distinct zones of sediment persistence in the watershed (Czuba and Foufoula-Georgiou, 2014, 2015). To investigate the role of network structure vs. the spatial distribution of sediment inputs on pulse evolution, a model run using spatially-uniform sediment inputs (Run 1) is compared with one using sediment inputs constrained by a sediment budget (Run 2). In-channel storage was added into the system and then higher-magnitude sediment pulses introduced on top of background sediment inputs, first at a single location (Run 3) and then throughout the system (Run 4). The run with a single sediment pulse at a discrete location (Run 3) is used to illustrate how downstream patterns of transport capacity can affect sediment pulse evolution. The run with a system-wide sediment pulse (Run 4) is used to investigate how both spatial patterns of transport capacity and network geometry affect sediment pulse evolution.

3.1. Site location

The Blue Earth River joins with its two main tributaries, the Le Sueur and Watonwan Rivers, shortly before entering the Minnesota River in Mankato, MN, USA (Fig. 2). Collectively, these three basins compose the Greater Blue Earth River (GBER) basin, covering 9200 km^2 of land historically in prairie but now 85% agriculture. The Minnesota River itself occupies a deeply-incised valley carved from the drainage of glacial Lake Agassiz at the end of the last glaciation. The incision of the Minnesota River valley led to the creation of upstream-migrating knickpoints on all major tributaries, leaving deeply-incised lower valleys ("knickzones") fed by rivers originating in low-gradient agricultural uplands (Gran et al., 2011a, 2011b). Bedload is derived from upland erosion and inputs from bluffs, streambanks, and ravines, particularly in the incised knickzones. On a specific sediment yield (Mg km^{-2} y^{-1}) basis, sediment derived from upland fields is small. Bluffs, on the other hand, occupy less than 1% of the landscape yet contribute the vast majority of the sediment load (Belmont et al., 2011; Bevis, 2015).

Most of the bed material load in the GBER is sand-sized. Gravel and cobbles are sourced primarily through incision into thick glacial tills with interbedded glaciofluvial sediments, leading to an increase in gravel and cobble abundance with increasing depth of incision downstream (Gran et al., 2013). The middle to lower reaches of the mainstem channels in the GBER basin thus have predominantly sandy bedload moving over an increasingly coarser bed downstream. Under these circumstances, sandy sediment pulses to the channel can translate downstream with minor dispersion (Lisle et al., 2001; Lisle, 2008; Sklar et al., 2009). In addition, because the knickzone valley is so confined, very little floodplain accommodation space exists (Belmont et al., 2011), allowing bedload to transport downstream with minimal attenuation due to storage. The model employed here is capable of capturing this behavior well (Czuba and Foufoula-Georgiou, 2014, 2015).

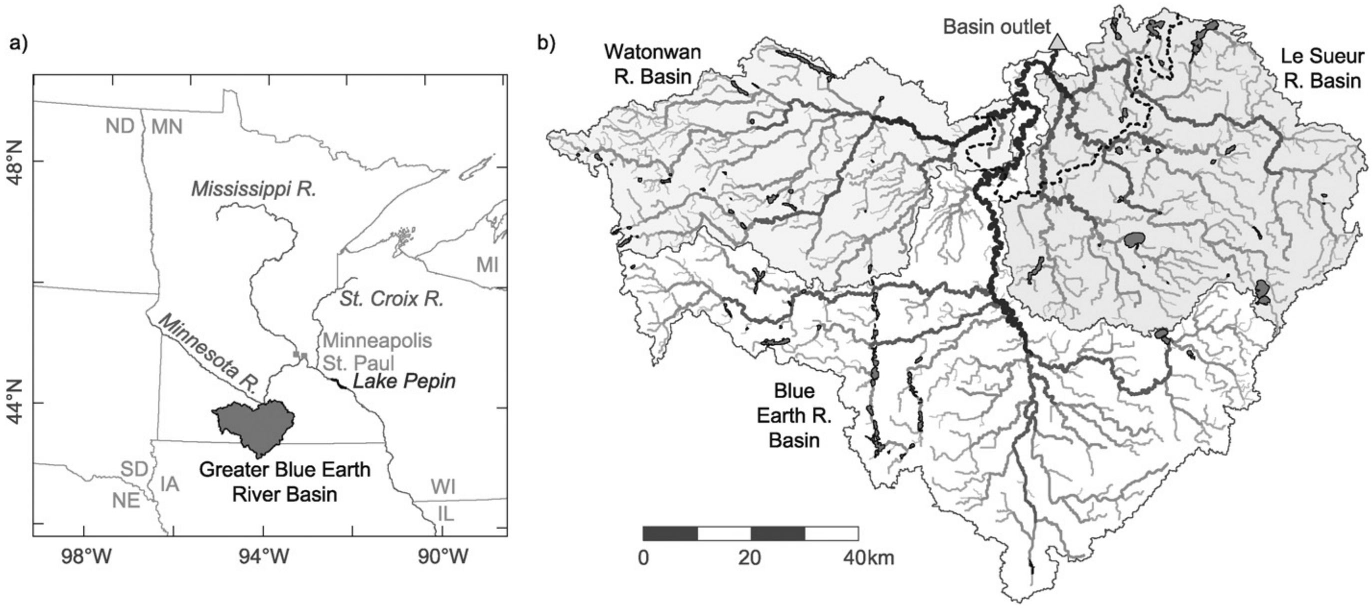

Fig. 2. Study area map. (a) Location map of the Greater Blue Earth River Basin in Minnesota and Iowa. (b) Detailed basin map showing major subbasins (Le Sueur, Blue Earth, and Watonwan), the channel network, lakes incorporated into the model, and the approximate extent of the knickzone (dashed line). Reaches of the channel network with larger upstream drainage areas are darker/thicker and with smaller upstream drainage areas are lighter/thinner.

3.2. Bed-material sediment model of the greater blue earth river basin

The model formulation described here advances the network-transport framework of Czuba and Foufoula-Georgiou (2014, 2015) which involves (1) decomposing the landscape into a connected network of elements including river channels and lakes, (2) spatially and temporally distributing sediment inputs, and (3) tracking these inputs through individual landscape elements via process-based time delays. Here this framework is advanced by including recurrent inputs informed by a sediment budget and also including lake and in-channel storage with direct feedback between in-channel storage and channel slope.

3.2.1. River network

The underlying structure of the model is the river network, obtained from the National Hydrography Dataset Plus Version 2 (NHDPlus V2) (McKay et al., 2012; HorizonSystems, 2014). The NHDPlusV2 network was preprocessed in ArcGIS by (1) clipping to the extent of the GBER basin; (2) removing isolated and secondary channels; (3) establishing a new set of links with index *i*, with a link defined either between tributary junctions, as the intersection of a lake with the network, or between a lake and a junction; and (4) mapping or computing attributes for each link from the original NHDPlusV2 network. The resulting network is composed of links representing river channels and lakes each with a set of unique attributes (Fig. 2b). For instance, each river channel contains the following attributes: index of link *i*, index of downstream link, link length ℓ_i, directly contributing area a_i, upstream drainage area A_i (i.e., the sum of a_i for all links upstream of and including link *i*), elevation at the upstream end of the link $\eta_{i,t}$, and channel slope $S_{i,t}$ (where all slopes less than 0.00001 were set to this value). Both $\eta_{i,t}$ and $S_{i,t}$ are allowed to change as a function of time, and thus include a subscript *t*.

3.2.2. Inputs from a sediment budget

A detailed sediment budget was compiled in the study area, first in the Le Sueur River basin (Belmont et al., 2011) and then expanded to include the entire GBER basin (Bevis, 2015) to better constrain the location, magnitude, and frequency of sediment inputs from four major sources: bluffs, streambanks, ravines, and uplands (dominated by low-gradient agricultural fields). Only inputs from bluffs, ravines, and uplands are incorporated into the present model as incorporating streambank exchange dynamics is beyond the scope of this study. An individual input from a bluff, ravine, or upland is referred to as a parcel, a fundamental unit transported on the network representing a collection of particles that are physically treated as a coherent unit. Each parcel is given a volume based on the volume eroded from a given feature. Although the original sediment budgets of Belmont et al. (2011) and Bevis (2015) were developed for fine sediment (silt and clay), grain size distributions measured for all source areas allow for the calculation of inputs of sand as well as silt and clay. Gravel remains a small portion of the total bedload and is not tracked here.

Bluffs are defined as along-channel features that exceed the height of the active floodplain. Bluffs were identified from a 3 m lidar DEM (digital elevation model) as areas that line active channels and have >3 m of relief over a 9 m × 9 m moving window. Bluffs in the GBER basin reach up to 70 m in height and occupy about 50% of the active channel corridor in the knickzone. Nearly 3500 individual bluffs were mapped in the GBER basin (Fig. 3a), each with its own characteristic attributes. Based on these attributes, the mass erosion rate of sand from each bluff ($M_{s,b}$ in Mg/y.; where the subscript *s* denotes sand and the subscript *b* denotes a bluff) was calculated as

$$M_{s,b} = e_b A_b f_{s,till} \rho_{till} \quad (1)$$

where e_b is the average subbasin-wide erosion rate in m/y determined through repeat aerial photo analysis of bluff crests between 1938 and 2005 or 2008 as described in Day et al. (2013) and Bevis (2015), A_b is the individual bluff surface area in m^2 (see Fig. 3a), $f_{s,till}$ is the fraction of sand in the till (0.35), and ρ_{till} is the average bulk density of the till (1.8 Mg/m^3). Bluff surface area is defined as the bluff area, connected to the river, projected onto a vertical plane. Long-term sub-basin average bluff erosion rates (e_b) varied from 0.05 to 0.25 m/y. (Day et al., 2013; Bevis, 2015). The total mass erosion rate of sand from all bluffs in the GBER basin was computed as 270,000 Mg/y.

Ravines are steep ephemeral channels that connect the low-gradient uplands to deeply-incised valleys. Ravines contribute the most sediment during high-magnitude precipitation events in spring and early summer, before crops are fully established. By late summer, ravines often run dry. Incised ravine areas were mapped throughout the GBER

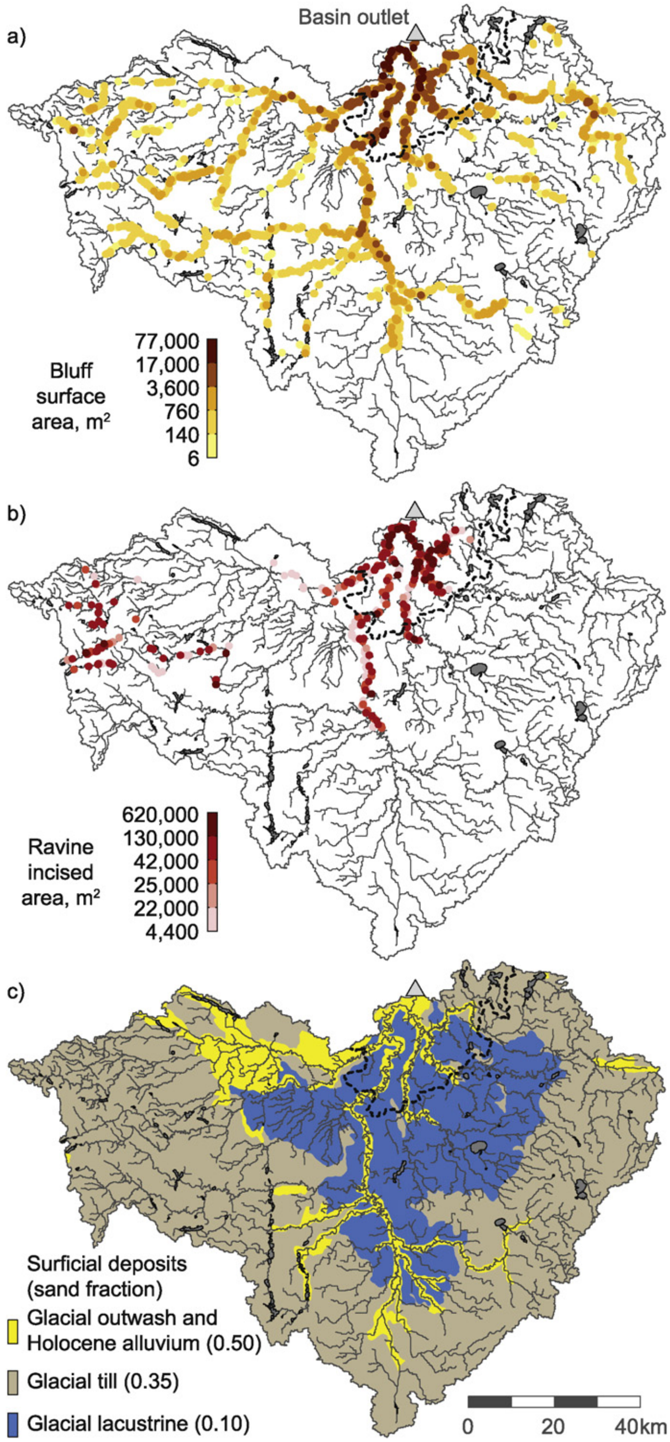

Fig. 3. Sediment budget features incorporated into the model. (a) Bluff locations colored by bluff surface area. (b) Ravine locations colored by ravine incised area. (c) Surficial deposits and sand fraction. The approximate extent of the knickzone is shown as a dashed line.

basin from 3 m aerial lidar data. Monitoring studies on five ravines in the lower Le Sueur River basin were used by Belmont et al. (2011) to determine an average annual ravine yield. Nearly 340 individual ravines were mapped in the GBER basin (Fig. 3b), each with its own characteristic attributes. Based on these attributes, the mass erosion rate of sand from each ravine ($M_{s,r}$ in Mg/y; where the subscript r denotes a ravine) was calculated as

$$M_{s,r} = A_r Y_r f_{s,till} \tag{2}$$

where A_r is the incised area of an individual ravine in m^2 (see Fig. 3b) and Y_r is the annual incised ravine yield (0.0034 Mg m^{-2} y^{-1}). The total mass erosion rate of sand from all ravines in the GBER basin was computed as 24,000 Mg/y.

Upland sediment yield was originally determined through analysis of total suspended solids (TSS) loads measured at gages located at the upper end of the knickzone in two tributaries of the Le Sueur River basin. Each TSS load was combined with sediment fingerprinting work by Belmont et al. (2011) to determine a load coming specifically from uplands, and then divided by upstream basin area to calculate a sediment yield (Y_u; where the subscript u denotes an upland). It includes sediment shed from agricultural fields as well as the ditch network.

There are as many uplands as there are links in the network (1360) with each upland area associated with a specific link. The mass erosion rate of sand from each upland area ($M_{s,u}$ in Mg/y) was calculated as

$$M_{s,u} = a_i Y_u f_{s,soil} \tag{3}$$

where a_i is the upland area or incremental contributing area to link i in m^2, Y_u is the annual upland yield (0.00002 Mg m^{-2} y^{-1}), and $f_{s,soil}$ is the fraction of sand in the soil (either 0.10 for glaciolacustrine deposits, 0.35 for glacial till, or 0.50 for glacial outwash and Holocene alluvium; STATSGO2 (2015), see Fig. 3c). The total mass erosion rate of sand from all uplands in the GBER basin was computed as 57,000 Mg/y.

3.2.3. Transport on the network

Individual parcels were transported through river channels according to process-based time delays. The in-channel travel time for a parcel to move through a given channel link was based on an analysis of sand transport assuming: (1) uniform (normal) flow hydraulics; (2) that Engelund and Hansen's (1967) sediment-transport formula represents the sand-transport process (neglecting the shear stress partition for bedforms); (3) hydraulic geometry scaling of streamflow depth, width, and velocity; (4) an intermittency of flows that transport the majority of sediment; (5) that sediment supply does not exceed transport capacity (these dynamics are handled mechanistically as a storage delay as described in Section 3.2.4); and (6) that sediment does not enter long-term floodplain storage. An overview schematic of this formulation is presented in Czuba and Foufoula-Georgiou (2015) and a detailed discussion of the formulation and its limitations is described in Czuba and Foufoula-Georgiou (2014). The river network and sediment inputs were delineated in ArcGIS with the routing model run in Matlab.

The essence of the sand-transport formulation is that the travel time t_i of a sand parcel to move through a channel link was computed as the time it takes to move through a link of length ℓ_i at a bulk sand transport velocity $u_{s,i}$ as

$$t_i = \frac{\ell_i}{u_{s,i}}. \tag{4}$$

The bulk sand transport velocity $u_{s,i}$ was obtained by decomposing the volumetric transport rate of sand $Q_{s,i}$ into a velocity and two length scales as

$$Q_{s,i} = u_{s,i}(\theta H_i)B_i, \tag{5}$$

where H_i is the channel depth of link i, B_i is the channel width of link i, and θ is a scale factor such that together (θH_i) defines a characteristic vertical length scale for sand transport where the majority of sand transport occurs ($\theta = 0.1$ for the GBER basin assuming the majority of sand transport occurs in the lower 10% of the flow depth).

Upon combining equations for channel hydraulics, sand transport, volumetric transport rate of sand, downstream hydraulic geometry at the two-year recurrence interval flow, the intermittency of the two-year recurrence interval flow, and parameters specific to the GBER basin (e.g., a bed-material grain size of 0.4 mm), the travel time t_i of a sand parcel to move through a channel link is given by

$$t_i = 18\ell_i A_i^{-0.285} S_i^{-3/2}. \tag{6}$$

The dependence of t_i on upstream drainage area A_i emerges from the hydraulic geometry scaling of flow velocity and depth, and on slope S_i from Engelund and Hansen's (1967) sediment-transport formula with dimensionless bed shear stress computed as the depth-slope product. Given that this travel time formulation neglects storage effects, Eq. (6) thus provides the fastest timescale for sand to move through a given channel reach. Storage was then included by incorporating additional delays to the travel time as described in Section 3.2.4.

3.2.4. Storage

Lake and in-channel storage was included in the model. Lakes were obtained from the waterbody feature of the NHDPlusV2 dataset (McKay et al., 2012; HorizonSystems, 2014). Only lakes that intersected the GBER network with surface area > 0.04 km^2 were incorporated into the network as individual links (Fig. 2b, defined as the segment(s) of the NHD network that intersected the lake. Trapping efficiencies for fine sediment were calculated using a relationship between upstream drainage area and lake volume (Brown, 1943). The average fine sediment trapping efficiency for lakes included in the model was 91%, thus lakes were assumed to have a 100% trapping efficiency for sand. Any sand parcels that entered a lake were removed from the system.

In-channel storage affected channel slope and thus transport. In-channel storage was accomplished by tracking the transport capacity of each link. In the sand-transport formulation (Section 3.2.3), a bulk transport velocity was derived by decomposing the volumetric transport rate of sand (at capacity) into a velocity and two length scales (Eq. (5)). As this derivation is based on at-capacity transport, the volume of sediment χ_i that can be moved at any one time at transport capacity through a link i falls directly out of the formulation as.

$$\chi_i = B_i(\theta H_i)\ell_i. \tag{7}$$

Whenever the total parcel volume in a given link was greater than χ_i, some parcels were brought into in-channel storage. The parcels that were the first in (following first in last out), and whose volumes brought the total parcel volume in a given link above capacity, were placed into storage by "freezing" those parcels' transport through the link. Once parcels exited the link, then additional parcels may be selected from storage (following last in first out) but only enough parcels to not exceed transport capacity. This "freezing" of parcels above capacity results in an additional time delay to the travel time of a parcel through a link due to transport limitations associated with transient storage.

As storage occurred, it affected the transport rate through feedbacks with channel slope. The volume of sediment in storage in link i was used to adjust the bed elevation $\eta_{i,t}$ at the upstream end of the link assuming a porosity of 0.4 (Wu and Wang, 2006). The storage volume was "placed" in one, two, or three wedges depending on the links directly upstream from link i. One wedge was located in link i, pinned at the downstream end, and its elevation was only adjusted at the upstream end. Additional wedges (one or two) were located in upstream channel links if those channel links existed; the elevation of the wedge in upstream links was only adjusted at the downstream end and was pinned at the upstream end. This storage dynamic increased the channel slope $S_{i,t}$ of the link with sediment in storage and decreased the slope of channel links directly upstream. The change in slope affects the travel time t_i via Eq. (6), but in the current formulation does not affect the volume of sediment transported at capacity χ_i. Thus, in-channel storage is allowed to increase (and decrease) the speed at which parcels moved through a given channel link, with effects propagating into channel links directly upstream.

Any parcels placed into in-channel storage were capable of being released from storage allowing the bed to return to its initial profile. However, new sediment inputs were not generated from the bed during supply-limited conditions. Instead, the bed was assumed to be armored at its initial profile with a coarse glacial lag and simulations then captured the dynamic of sand moving over a non-erodible substrate.

3.3. Overview of simulation scenarios

Four different scenarios were simulated in the model to examine how the spatial pattern of transport capacity and network geometry affect sediment pulse evolution through the GBER watershed (Table 1). Each scenario had temporally-recurrent sediment inputs where the interarrival time of each input was randomly selected from an exponential distribution with a mean of one year (to align with annualized sediment budget input volumes). The time step in the model was 18.25 days so that 20 time steps yielded one year. Inputs were first added at time 0 years and it took roughly 100 years to "prime" the basin with inputs. That is, it took roughly 100 years for an input at the farthest location to exit the basin at the outlet, and in this amount of time much of the initial bed aggradation had stabilized.

A few minor items needed to be addressed before model simulations could begin. The effect of Rapidan Dam, located on the Blue Earth River between the Watonwan and Le Sueur River tributaries, was removed by selecting a channel slope for the links upstream and downstream of the dam that linearly connected the bed elevations between unaffected upstream and downstream points. Because a minimum slope of 0.00001 was enforced throughout the network, bed elevations were recomputed from the basin outlet in order to establish consistency between $\eta_{i,t}$ and $S_{i,t}$. A lower limit for transport capacity was set at 50 m^3. A maximum parcel volume was set to half the lower limit of transport capacity at 25 m^3 and any instantaneous sediment inputs >25 m^3 were split into equal volumes of <25 m^3. Due to the presence of some very short links in the network (<300 m) that arose between closely-spaced tributaries, some links had a very small capacity resulting in an artificial "bottleneck" in the network. To circumvent this issue, a minimum capacity for these short links was set as the maximum of (1) the capacity of the link computed via Eq. (7), (2) the capacity of directly upstream links, or (3) 100 m^3.

Descriptions of the four different model scenarios (Table 1) are as follows:

- *Scenario 1* (*spatially-uniform inputs, no in-channel storage*): A spatially-uniform input was applied to the network such that the long-term average input rate matched that of the sediment budget (350,000 Mg/y; sum of bluff, ravine, and upland inputs). To the upstream end of each link, temporally-recurrent inputs were introduced each with a mass of $a_i \times 38$ Mg y^{-1} km^{-2} (350,000 Mg/y per basin area of 9200 km^2) with an interarrival time of one year.
- *Scenario 2* (*sediment budget inputs, no in-channel storage*): This scenario was the same as scenario 1 except that it aligned the sediment inputs with the sediment budget. Temporally-recurrent inputs were added to the network at the locations of bluffs, ravines, and uplands as the long-term average rates generated by each specific feature as described in Section 3.2.2.
- *Scenario 3* (*sediment budget inputs, in-channel storage, single pulse*): As in scenario 2, temporally-recurrent inputs were added to the network at the locations of bluffs, ravines, and uplands as the long-term average rates generated by each specific feature according to the sediment budget. After 100 years of simulation, a single pulse was introduced to the upstream end of one link in the network with a volume equal to 4× its capacity (4χ_i or 42,000 m^3).
- *Scenario 4* (*sediment budget inputs, in-channel storage, distributed pulse*): The spatial and temporal characteristics of the background inputs were the same for this scenario as for scenario 3. After 100 years of simulation, a distributed pulse was introduced to the upstream end

Table 1
Descriptions of model scenarios.

Scenario	Sediment Inputs			In-channel storage[1]	Pulse	Run time (y)
	Spatial	Temporal	Volumes			
1	uniform	exponential interarrival times	equal volumes	no	none	100
2	sediment budget	exponential interarrival times	dictated by sediment budget	no	none	100
3	sediment budget	exponential interarrival times	dictated by sediment budget	yes	single pulse	300
4	sediment budget	exponential interarrival times	dictated by sediment budget	yes	distributed to all links	600

[1] All scenarios included lake storage.

of every link in the network each with a volume equal to 2× its capacity ($2\chi_i$) for a total input volume distributed throughout the basin of 9,600,000 m^3.

Note that mass of sediment is interchanged into volume of sediment through a sediment density of 2.65 Mg/m^3, and a bed sediment porosity of 0.4 is applied when adjusting bed elevations. For both scenarios 3 and 4, an equivalent baseline simulation without the added pulse was used to difference bed elevations of the pulse simulation from those of the background variability captured in the baseline simulation in order to isolate the effects of the pulse. Additionally, the parcels composing the pulse were "tagged" to see how they moved through the system independent of their effect on bed elevations.

4. Results and discussion

4.1. Modeling scenarios 1 and 2: No sediment pulse

After a 100 year simulation period for scenarios 1 and 2, the resulting bed sediment depths were mapped throughout the GBER basin (Fig. 4). Despite the difference in the spatial distributions of inputs, the "hotspots" of relatively thicker bed sediment depths between the two scenarios are largely the same. This was discussed in Czuba and Foufoula-Georgiou (2015), which only considered uniform inputs, but even with the sediment budget inputs the same "hotspots" emerge. While most sediment is generated in the knickzone, there are many bluffs (which are the largest contributors of sediment) that line the major rivers throughout the network (Fig. 3a). This results in a pattern of relative sediment depths along mainstem rivers similar to the hierarchical ordering that arises with uniform inputs. The spatial pattern of sediment depths is driven by a combination of spatial pattern of inputs, hierarchical ordering by the network geometry, and local channel characteristics that dictate how sediment can move through a given reach.

The magnitude of the sediment depths that emerge from scenarios 1 and 2 is different, however. For both scenarios 350,000 Mg/y. of sand on average is added to the network, either distributed uniformly (Fig. 4a) or according to the sediment budget (Fig. 4b). In the GBER basin, most of the sediment is generated in the knickzone where rivers are steeper and have a larger capacity to effectively transport these large inputs of sediment downstream to the Minnesota River. In effect, when this sediment is input according to the sediment budget, the largest bed sediment depths are around 1 m and elsewhere become very small at 2 mm for the 0.75 quantile. If instead that same input is delivered uniformly, the upland reaches receive much more sediment than the budget specifies where the largest bed sediment depths remain around 1 m but the bed sediment depths throughout the basin increase to 10 mm for the 0.75 quantile. These higher bed sediment depths throughout the basin for the uniformly-distributed magnitude/pattern of inputs as compared with the sediment budget inputs, reflects the redistribution of the simulated sediment supply from concentrated within the knickzone to dispersed throughout the entire basin.

The spatial pattern of sediment depths, while unique to each watershed, affects how the network handles a sediment pulse moving through it. Many of the reaches with high sediment depths tend to be the same reaches where storage will occur during passage of a sediment pulse, either because the transport capacity is low or the volume of background inputs (due to the geometry of tributary inputs) is high.

4.2. Modeling scenarios 3 and 4: sediment pulse

Scenarios 3 and 4 investigate how sediment pulses evolve within a network context. Results for scenario 3 are presented along a single pathway through the network that initiates in Elm Creek, a tributary to the Blue Earth River (Fig. 5a). The transport capacity (Eq. (7)) of the channel along this pathway generally decreases downstream until it

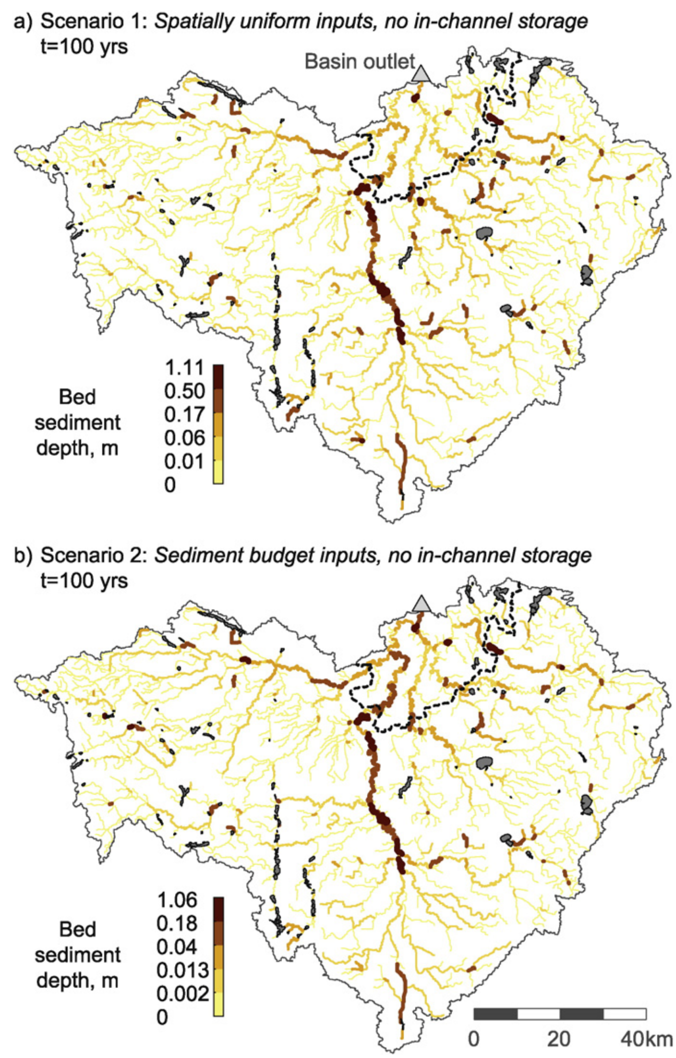

Fig. 4. Bed sediment depths throughout the Greater Blue Earth River Basin after 100 years of simulation for (a) scenario 1 with spatially-uniform inputs and (b) scenario 2 with sediment budget inputs, both with no in-channel storage. The color breaks are at the 0.99, 0.95, 0.90, and 0.75 quantile for each scenario. The approximate extent of the knickzone is shown as a dashed line.

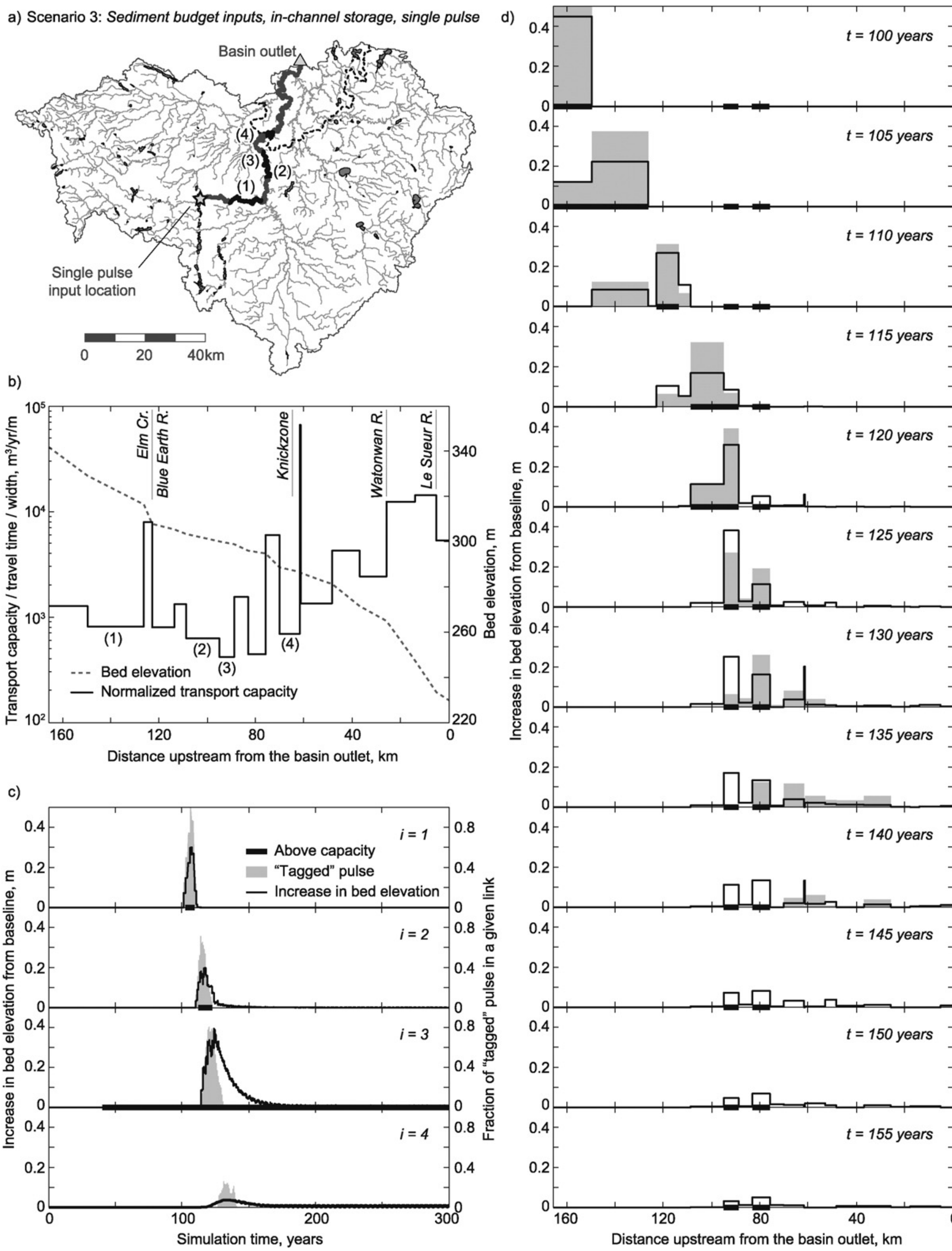

Fig. 5. Response of the Greater Blue Earth River Basin to a single sediment pulse input for scenario 3. (a) Map of the Greater Blue Earth River Basin showing the location of the single pulse input (star) on Elm Creek and the pathway from that point to the outlet. The approximate extent of the knickzone is shown as a dashed line. (b) Normalized transport capacity and bed elevation along the pathway from the input location to the outlet. Tributary junctions are noted for reference. Increase in bed elevation from baseline and progression of the “tagged” pulse (c) at four locations through time and (d) along the pathway from the input location to the outlet at twelve instants in time. The numbers in (a) and (b) correspond to the four locations in (c).

reaches a minimum roughly 90 km upstream from the outlet (Fig. 5b). From this point to the outlet, the transport capacity generally increases as the channel steepens within the knickzone.

Along this pathway, bed elevation is tracked, both in terms of the increase above baseline conditions and the sediment pulse parcels themselves. At four different locations, the increase in bed elevation from baseline and the location of the “tagged” pulse through time shows that the input sediment moved on the leading edge of the bed elevation “wave” (Fig. 5c). There is an extra increase in bed elevation in some reaches beyond that directly produced by the input pulse. This occurs because once a large volume of sediment enters a given reach, it “freezes” the transport of the background sediment moving through that reach while the pulse overrides this material now in storage. Once the pulse has left the reach the background supply continues to add sediment to the reach, so the reach now has to move the background supply in addition to the sediment emerging from storage. This effect greatly enhances the impact of a single large sediment pulse on bed elevation.

When the evolution of the single large sediment pulse is viewed spatially, there is a mixture of pulse translation and dispersion (Fig. 5d). Where the transport capacity is gradually decreasing downstream (from 160 to 100 km upstream from the basin outlet), the pulse largely translates with slight dispersion; the increase in bed elevation is coincident with the “tagged” pulse. Once the pulse reaches the minimum transport capacity along the pathway (around 90 km upstream from the basin outlet), the pulse largely disperses in place because of this local “bottleneck” in the system. It is at this point that the increase in bed elevation and the “tagged” pulse decouple as the pulse sediment moves downstream while bed elevations in the low capacity reach are still responding to the legacy of the increased supply. This particular pattern arises in part due to the sediment accounting and the use of transient in-channel vs. long-term (floodplain) storage.

Once a reach exceeds transport capacity the additional time delay due to storage effects can create a considerable difference in the timing of the pulse sediment compared to the travel time due to at-capacity transport. For instance, the initial pulse was 4× the transport capacity of the reach to which it was emplaced. This reach had an at-capacity transport time of about 2 years, but due to the pulse, the travel time increased by a factor of 4 through this reach to about 8 years (time to arrive at link $i = 1$, Fig. 5c). Farther downstream the at-capacity transport time to arrive at link $i = 4$ was about 22 years, however, it took roughly twice that time for the maximum effect of the pulse to occur. The additional storage delay generally became longer for reaches in close proximity to the input location and decreased farther downstream. This effect is controlled by the volume of the pulse relative to the transport capacity, which was highest at the source, and also due to the increase in the absolute capacity from an increase in channel width, particularly once Elm Creek entered the Blue Earth River.

Scenario 4 shows how the river network responds when the entire network is subjected to a pulse such that twice the capacity of each link is added on top of the background rate (Fig. 6). For each link in the network, the fraction of time spent above capacity during the 500 year period following the pulse input generally shows the same “hotspot” locations as identified from bed sediment depths, with a few distinct differences (see Figs. 4 and 6a). There is a band of major river reaches with a relatively larger time spent above capacity just upstream of the knickzone. These locations become bed-material “bottlenecks” where transport capacity along a given river is at its lowest just before having an increased capacity downstream in the knickzone. Reaches just upstream of the knickzone may be most susceptible to aggradation and potentially accelerated channel migration (such as suggested by Czuba and Foufoula-Georgiou (2015)), due to a large increase in upstream bed material sediment supply. In addition, reaches within the knickzone spend less time above capacity, even though earlier runs (Fig. 4) indicate that these areas have a lot of bed-material load entering. Once storage is incorporated into the model, the “bottlenecks” upstream of the knickzone, coupled with the increasing transport capacity through the knickzone mean that these reaches in the knickzone are readily able to transport any sediment released from reaches directly upstream. This emphasizes the importance of the spatial pattern of relative transport capacity in the network.

Due to the larger total volume and spatially-distributed nature of the pulse for scenario 4, the time scales of sediment persistence in the system are much longer than for the single isolated pulse of scenario 3. As a way to show a two-dimensional network on a one-dimensional space, a network width function was calculated (Fig. 6d), which describes the fraction of links a given distance from the basin outlet (where distances are taken along the network; for more information see Czuba and Foufoula-Georgiou, 2014, 2015). An extension of this concept involves creating a network width function of the “tagged” pulse (Fig. 6e), which shows where the dispersed sediment pulse is located with respect to distance from the basin outlet. The correspondence between the network width function of the “tagged” pulse (Fig. 6e) and the locations of the “tagged” pulse on the network itself is shown at 105 and 150 years (Fig. 6b and c, respectively). Within the knickzone (for locations roughly <50 km from the basin outlet), the excess sediment is quickly flushed through these reaches within about 10 years (Fig. 6e). The locations where the sediment pulse persists the longest are generally the same “hotspots” identified previously (Fig. 6c and e). In this scenario the “tagged” pulse persists in the network for well over 100 years after its injection, whereas the increase in bed elevation (not shown) persists for much longer.

4.3. Role of network structure on sediment connectivity

The scenarios reviewed above illustrate the importance of network structure, including both network geometry and the spatial pattern of transport capacity, on pulse behavior. In the absence of storage, sediment in the GBER model would tend to translate downstream as seen in Fig. 5d from 100 to 160 km upstream. Incorporating storage into the system had the effect of dispersing the pulse in reaches where sediment inputs exceeded the transport capacity of an individual link. The spatial structure of the GBER network created sediment “bottlenecks” just upstream of the knickzone. These low-capacity reaches then feed a reduced load downstream, where increased slope readily moves sediment down to the mouth of the river. These low-capacity reaches can have considerable control of the sediment signal at the outlet.

The effect of low-capacity reaches differs based on the volume of sediment moving through the system. If all reaches are under-capacity, even with a sediment pulse, then dispersion associated with storage effects will be minimal. As either the pulse volume or the background bed material load increases, however, more reaches will hit capacity, sediment will move into storage, and the pulse itself will begin to disperse. Although this model only included in-channel storage, floodplain storage would tend to have an even greater effect on delaying release of sediment downstream, lengthening the time required for the sediment pulse to move through the network, as seen in field cases with legacy sediments (James, 1989, 1991, 2010; Lisle, 2008).

There are two main elements that dictate whether or not a reach will be over-capacity: the capacity of the reach itself and the influx of sediment to that reach. Sediment inputs arriving in unison at tributary junctions can overwhelm the transport capacity of a reach, inducing local storage. The maps in Fig. 4 show where sediment amasses due to tributary interactions synchronizing sediment inputs. In the absence of storage, sediment collecting in these reaches can move downstream as a larger wave. Other studies have found that widely-dispersed sediment pulses translating downstream can produce or maintain sediment waves at the mouth when sediment inputs synchronize at tributary junctions (Jacobson, 1995; Jacobson and Gran, 1999; Benda et al., 2004a; Czuba and Foufoula-Georgiou, 2014, 2015). With storage, however, low-capacity reaches lead to the “bottlenecks” seen in scenarios 3 and 4, and ultimately dispersion of the sediment pulse. Thus, the integrity of the sediment pulse is a function of the total load moving through a network, how close to capacity individual reaches are, and the likelihood that the extra sediment associated with the pulse will go into transient or long-term storage.

Overlain on the pulse modifications associated with network structure are the reach-scale processes reviewed earlier that would tend to translate or disperse a sediment pulse. Results from field and flume have shown that most sediment pulses tend to disperse. Over

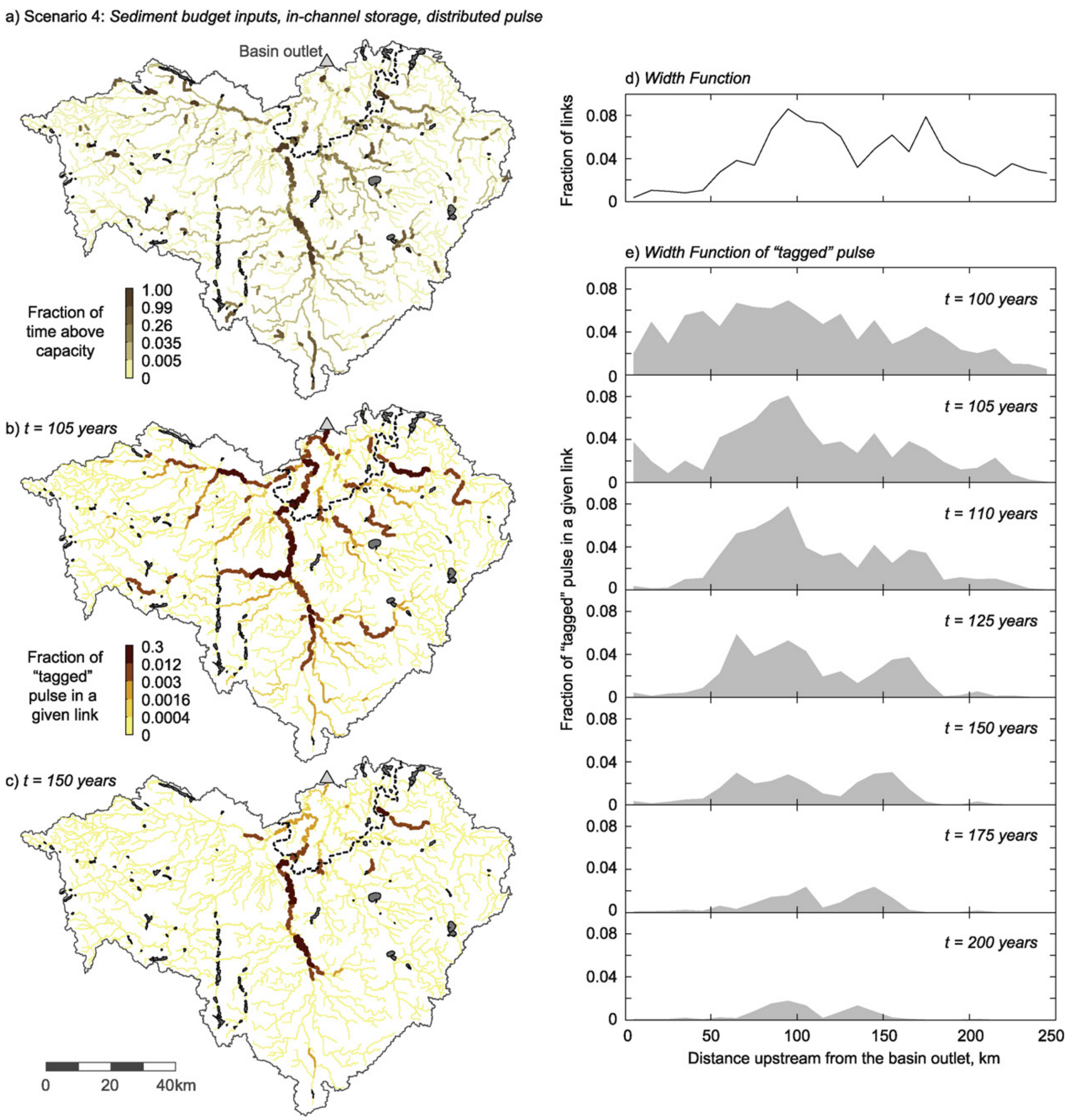

Fig. 6. Response of the Greater Blue Earth River Basin to a distributed sediment pulse input for scenario 4. (a) Map of the Greater Blue Earth River Basin showing the fraction of time a given link was above capacity for a period of 500 years after pulse input. The color breaks are at the 0.99, 0.95, 0.90, and 0.75 quantile. The approximate extent of the knickzone is shown as a dashed line. Map of the fraction of the "tagged" pulse throughout the network at (b) 105 years and (c) 150 years. (d) Network width function describing the fraction of links a given distance from the basin outlet. The width function maps a two-dimensional network onto a one-dimensional space (for more information see Czuba and Foufoula-Georgiou, 2014, 2015). (e) Network width function of the "tagged" pulse at various times showing where the dispersed sediment pulse is located with respect to distance from the basin outlet. The knickpoint is located approximately 45–65 km upstream from the outlet.

time, studies have constrained the conditions under which significant components of translation are observed: low Froude number flows, fine sediment overlying a coarse bed, and small inputs of sediment with only minor or no effect on the flow field. The network-routing model developed in the GBER does allow for significant translation, in part because the sediment is sand-sized, moving over a coarse bed, with little storage in the knickzone. Channels where this is not the case would likely show greater dispersion outside of the low-capacity reaches. In this case, the dispersive effects of storage would enhance this behavior, and the ability of sediment to synchronize at tributary junctions would remain the main driver for maintaining pulse integrity.

5. Concluding remarks

- Research to date has shown that most sediment pulses, particularly in gravel-bed rivers, tend to disperse more than translate at a reach-scale. Fine-grained pulses travelling over a coarse-grained bed, with low Froude number flows and small volumes tend to have the greatest components of translation at a reach-scale (Lisle et al., 1997, 2001; Sutherland et al., 2002; Cui and Parker, 2005; Cui et al., 2005; Lisle, 2008; Sklar et al., 2009; Venditti et al., 2010a; Humphries et al., 2012).
- Network structure must be taken into consideration at the watershed scale to evaluate how a sediment pulse evolves downstream. Depending on the network geometry, tributary junctions can lead to

synchronization of pulses, causing wave-like pulses to develop and move downstream. Thus, spatially-distributed perturbations can lead to the development of sediment waves through network interactions (Jacobson, 1995; Jacobson and Gran, 1999; Benda and Dunne, 1997a; Benda et al., 2004a, 2004b; Czuba and Foufoula-Georgiou, 2014).

- The modeling work here shows the importance of both network geometry and the spatial pattern of relative transport capacity on maintaining sediment pulse integrity in a network. Sediment is more likely to enter storage in reaches with low transport capacities relative to upstream reaches. These sediment "bottlenecks" cause sediment pulses that would otherwise translate downstream to disperse in these zones. The sediment associated with the initial pulse can become dissociated from the bed elevation wave.
- The effect of storage on pulse behavior is a function of both the size of the pulse and the size of the background inputs entering a reach. If inputs are below capacity, leading to minimal or no pulse sediment going into storage, then there will be minimal dispersion. For greater pulse volume or greater background sediment loads, storage becomes more important, enhancing dispersion.
- Model simulations in the GBER basin, specifically, found that areas just upstream of the knickzone stayed above capacity longer than reaches downstream while responding to a sediment pulse. These reaches control the downstream movement of bed material load, dispersing the pulse and releasing lower volumes of sediment to downstream reaches where they readily translated through the system. The pattern of relative transport capacity on the network is thus a primary control on sediment pulse behavior at a watershed scale.

Acknowledgments

This research was funded by NSF grant EAR-1209402 under the Water Sustainability and Climate Program with additional funding for the sediment budget from the Minnesota Department of Agriculture through Minnesota's Clean Water Legacy Fund. JAC acknowledges support provided by an Interdisciplinary Doctoral Fellowship through the University of Minnesota's Graduate School and Institute on the Environment and by an Edward Silberman Fellowship through St. Anthony Falls Laboratory. The sediment budget was originally compiled by Martin Bevis, with bluff erosion rates measured by Stephanie Day and Girish Uprety. We appreciate the comments from Dr. Stephen Rice and one anonymous reviewer that helped improve this manuscript.

References

Bartley, R., Rutherfurd, I., 2005. Re-evaluation of the wave model as a tool for quantifying the geomorphic recovery potential of streams disturbed by sediment slugs. Geomorphology 64, 221–242. http://dx.doi.org/10.1016/j.geomorph.2004.07.005.

Belmont, P., Gran, K.B., Schottler, S.P., Wilcock, P.R., Day, S.S., Jennings, C., Lauer, J.W., Viparelli, E., Willenbring, J.K., Engstrom, D.R., Parker, G., 2011. Large shift in source of fine sediment in the upper Mississippi River. Environ. Sci. Technol. 45, 8804–8810. http://dx.doi.org/10.1021/es2019109.

Benda, L., Dunne, T., 1997a. Stochastic forcing of sediment routing and storage in channel networks. Water Resour. Res. 33, 2865–2880.

Benda, L., Dunne, T., 1997b. Stochastic forcing of sediment supply to channel networks from landsliding and debris flow. Water Resour. Res. 33, 2849–2863.

Benda, L., Andras, K., Miller, D., Bigelow, P., 2004a. Confluence effects in rivers: Interactions of basin scale, network geometry, and disturbance regimes. Water Resour. Res. 40, 1–15. http://dx.doi.org/10.1029/2003WR002583.

Benda, L., Miller, D., Bigelow, P., Andras, K., 2003. Effects of post-wildfire erosion on channel environments, Boise River, Idaho. For. Ecol. Manag. 178, 105–119. http://dx.doi.org/10.1016/S0378-1127(03)00056-2.

Benda, L., Poff, N.L., Miller, D., Dunne, T., Reeves, G., Pess, G., Pollock, M., 2004b. The Network Dynamics Hypothesis: How channel networks structure riverine habitats. Bioscience 54, 413. http://dx.doi.org/10.1641/0006-3568(2004)054[0413:TNDHHC]2.0.CO;2.

Bevis, M., 2015. Sediment budgets indicate Pleistocene base level fall drives erosion in Minnesota's greater Blue Earth River basin (M.S. Thesis) University of Minnesota Duluth: University of Minnesota Digital Conservancy http://hdl.handle.net/11299/170661.

Brown, C.B., 1943. Discussion of sedimentation in reservoirs. Proc. Am. Soc. Civ. Eng. 69, 1493–1500.

Church, M., 1983. Pattern of instability in a wandering gravel bed channel. Spec. Publ. Int. Assoc. Sedimentol. 6, 169–180.

Cui, Y., 2007. The unified gravel-sand (TUGS) model: Simulating sediment transport and gravel/sand grain size distributions in gravel-bedded rivers. Water Resour. Res. 43, 1–16. http://dx.doi.org/10.1029/2006WR005330.

Cui, Y., Parker, G., 2005. Numerical model of sediment pulses and sediment-supply disturbances in mountain rivers. J. Hydraul. Eng. 131, 646–656. http://dx.doi.org/10.1061/(ASCE)0733-9429(2005)131:8(646).

Cui, Y., Braudrick, C., Dietrich, W.E., Cluer, B., Parker, G., 2006. Dam Removal Express Assessment Models (DREAM). J. Hydraul. Res. 44, 308–323. http://dx.doi.org/10.1080/00221686.2006.9521683.

Cui, Y., Parker, G., Lisle, T.E., Gott, J., Hansler-Ball, M.E., Pizzuto, J.E., Allmendinger, N.E., Reed, J.M., 2003a. Sediment pulses in mountain rivers: 1. Experiments. Water Resour. Res. 39. http://dx.doi.org/10.1029/2002WR001803 (n/a–n/a.).

Cui, Y., Parker, G., Lisle, T.E., Pizzuto, J.E., Dodd, A.M., 2005. More on the evolution of bed material waves in alluvial rivers. Earth Surf. Process. Landforms 30, 107–114. http://dx.doi.org/10.1002/esp.1156.

Cui, Y., Parker, G., Pizzuto, J.E., Lisle, T.E., 2003b. Sediment pulses in mountain rivers: 2. Comparison between experiments and numerical predictions. Water Resour. Res. 39, 1–11. http://dx.doi.org/10.1029/2002WR001805.

Czuba, J.A., Foufoula-Georgiou, E., 2014. A network-based framework for identifying potential synchronizations and amplifications of sediment delivery in river basins. Water Resour. Res. 50, 2108–2123. http://dx.doi.org/10.1002/2013WR014227.

Czuba, J.A., Foufoula-Georgiou, E., 2015. Dynamic connectivity in a fluvial network for identifying hotspots of geomorphic change. Water Resour. Res. 51, 1401–1421. http://dx.doi.org/10.1002/2014WR016139.

Dadson, S.J., Hovius, N., Chen, H., Dade, W.B., Lin, J.C., Hsu, M.L., Lin, C.W., Horng, M.J., Chen, T.C., Milliman, J., Stark, C.P., 2004. Earthquake-triggered increase in sediment delivery from an active mountain belt. Geology 32, 733–736. http://dx.doi.org/10.1130/G20639.1.

Day, S.S., Gran, K.B., Belmont, P., Wawrzyniec, T., 2013. Measuring bluff erosion part 2: Pairing aerial photographs and terrestrial laser scanning to create a watershed scale sediment budget. Earth Surf. Process. Landforms 38, 1068–1082. http://dx.doi.org/10.1002/esp.3359.

East, A.E., Pess, G.R., Bountry, J.A., Magirl, C.S., Ritchie, A.C., Logan, J.B., Randle, T.J., Mastin, M.C., Minear, J.T., Duda, J.J., Liermann, M.C., McHenry, M.L., Beechie, T.J., Shafroth, P.B., 2015. Large-scale dam removal on the Elwha River, Washington, USA: River channel and floodplain geomorphic change. Geomorphology 228, 765–786. http://dx.doi.org/10.1016/j.geomorph.2014.08.028.

Engelund, F., Hansen, E., 1967. A monograph on sediment transport in alluvial streams. Tek. Forlag., Copenhagen, Denmark (62 p.).

Engstrom, D.R., Almendinger, J.E., Wolin, J.A., 2009. Historical changes in sediment and phosphorus loading to the upper Mississippi River: Mass-balance reconstructions from the sediments of Lake Pepin. J. Paleolimnol. 41, 563–588. http://dx.doi.org/10.1007/s10933-008-9292-5.

Ferguson, R.I., Church, M., Rennie, C.D., Venditti, J.G., 2015. Reconstructing a sediment pulse: modeling the effect of placer mining on Fraser River, Canada. J. Geophys. Res. Earth Surf. http://dx.doi.org/10.1002/2015JF003491.

Ferguson, R.I., Cudden, J.R., Hoey, T.B., Rice, S.P., 2006. River system discontinuities due to lateral inputs: Generic styles and controls. Earth Surf. Process. Landforms 31, 1149–1166. http://dx.doi.org/10.1002/esp.1309.

Fitzpatrick, F.A., Knox, J.C., Whitman, H.E., 1999. Effects of Historical land-cover changes on flooding and sedimentation, North Fish Creek, Wisconsin. USGS Water Resour. Investig. 99-4083, 1–12.

Gilbert, G.K., 1917. Hydraulic-mining debris in the Sierra Nevada. U.S. Geol. Surv. Prof. Pap. 105.

Gran, K.B., 2012. Strong seasonality in sand loading and resulting feedbacks on sediment transport, bed texture, and channel planform at Mount Pinatubo, Philippines. Earth Surf. Process. Landforms 37, 1012–1022. http://dx.doi.org/10.1002/esp.3241.

Gran, K.B., Montgomery, D.R., 2005. Spatial and temporal patterns in fluvial recovery following volcanic eruptions: Channel response to basin-wide sediment loading at Mount Pinatubo, Philippines. Bull. Geol. Soc. Am. 117, 195–211. http://dx.doi.org/10.1130/B25528.1.

Gran, K.B., Belmont, P., Day, S.S., Finnegan, N., Jennings, C., Lauer, J.W., Wilcock, P.R., 2011a. Landscape evolution in south-central Minnesota and the role of geomorphic history on modern erosional processes. GSA Today 21, 7–9. http://dx.doi.org/10.1130/G121A.1.

Gran, K., Belmont, P., Day, S., Jennings, C., Lauer, J.W., Viparelli, E., Wilcock, P., Parker, G., 2011b. An Integrated Sediment Budget for the Le Sueur River Basin. Final Report to the Minnesota Pollution Control Agency, wq-iw7-29o (128 p.).

Gran, K.B., Finnegan, N., Johnson, A.L., Belmont, P., Wittkop, C., Rittenour, T., 2013. Landscape evolution, valley excavation, and terrace development following abrupt postglacial base-level fall. Bull. Geol. Soc. Am. 125, 1851–1864. http://dx.doi.org/10.1130/B30772.1.

Hansler, M.E., 1999. Sediment wave evolution and analysis of a one-dimensional sediment routing model, Navarro River. Humboldt State University, Northwestern California.

Hassan, M., Church, M., Lisle, T.E., Brardinoni, F., Benda, L., Grant, G.E., 2005. Sediment transport and channel morphology of small, forested streams. J. Am. Water Resour. Assoc. 41, 853–876.

Hoffman, D.F., Gabet, E.J., 2007. Effects of sediment pulses on channel morphology in a gravel-bed river. Bull. Geol. Soc. Am. 119, 116–125. http://dx.doi.org/10.1130/B25982.1.

HorizonSystems, 2014. NHDPlus Version 2 [WWW Document]. Horiz. Syst. Corp., Herndon, VA (URL http://www.horizon-systems.com/NHDPlus/NHDPlusV2_home.php (accessed 5.20.14)).

Humphries, R., Venditti, J.G., Sklar, L.S., Wooster, J.K., 2012. Experimental evidence for the effect of hydrographs on sediment pulse dynamics in gravel-bedded rivers. Water Resour. Res. 48, 1–15. http://dx.doi.org/10.1029/2011WR010419.

Iseya, F., Ikeda, H., 1987. Pulsations in bedload transport rates induced by a longitudinal sediment sorting: A flume study using sand and gravel mixtures. Geogr. Ann. Ser. A. Phys. Geogr. 69, 15–27.

Jacobson, R.B., 1995. Spatial controls on patterns of land-use induced stream disturbance at the drainage-basin scale – An example from gravel-bed streams of the Ozark plateau. In: Costa, J.E., Miller, A.J., Potter, K.W., Wilcock, P.R. (Eds.), Natural and Anthropogenic Influences in Fluvial Geomorphology Geophysical Monograph 89. AGU, Washington, D.C., pp. 219–239.

Jacobson, R.B., Gran, K.B., 1999. Gravel sediment routing from widespread, low-intensity landscape disturbance, Current River basin, Missouri. Earth Surf. Process. Landforms 24, 897–917. http://dx.doi.org/10.1002/(SICI)1096-9837(199909)24:10<897::AID-ESP18>3.0.CO;2-6.

Jacobson, R.B., Primm, A.T., 1997. Historical land-use changes and potential effects on stream disturbance in the Ozark Plateaus, Missouri. U. S. Geol. Surv. Water Supply Pap. 2484, 85.

Jacobson, R.B., Femmer, S.R., McKenney, R.A., 2001. Land-use changes and the physical habitat of streams – a review with emphasis on studies within the U.S. Geological Survey Federal–State Cooperative Program. U.S. Geol. Surv. Cirrcular 1175, 74.

James, L.A., 1989. Sustained storage and transport of hydraulic gold mining sediment in the Bear River, California. Ann. Assoc. Am. Geogr. 79, 570–592. http://dx.doi.org/10.1111/j.1467-8306.1989.tb00277.x.

James, L.A., 1991. Incision and morphologic evolution of an alluvial channel recovering from hydraulic mining sediment. Bull. Geol. Soc. Am. 103, 723–736. http://dx.doi.org/10.1130/0016-7606(1991)103<0723:IAMEOA>2.3.CO;2.

James, L.A., 1993. Sustained reworking of hydraulic mining sediment in California: G.K. Gilbert's sediment wave model reconsidered. Z. Geomorphol. 88, 49–66.

James, L.A., 2010. Secular sediment waves, channel bed waves, and legacy sediment. Geogr. Compass 4, 576–598. http://dx.doi.org/10.1111/j.1749-8198.2010.00324.x.

Kasai, M., Marutani, T., Brierley, G.J., 2004. Patterns of sediment slug translation and dispersion following typhoon-induced disturbance, Oyabu Creek, Kyushu, Japan. Earth Surf. Process. Landforms 29, 59–76. http://dx.doi.org/10.1002/esp.1013.

Keefer, D.K., 1994. The importance of earthquake-induced landslides to long-term slope erosion and slope-failure hazards in seismically active regions. Geomorphology 10, 265–284. http://dx.doi.org/10.1016/0169-555X(94)90021-3.

Knighton, A.D., 1989. River adjustment to changes in sediment load: The effects of tin mining on the Ringarooma River, Tasmania, 1875-1984. Earth Surf. Process. Landforms 14, 333–359. http://dx.doi.org/10.1002/esp.3290140408.

Knighton, A.D., 1991. Channel bed adjustment along mine-affected rivers of northeast Tasmania. Geomorphology 4, 205–219. http://dx.doi.org/10.1016/0169-555X(91)90004-T.

Lewin, J., Bradley, S.B., Macklin, M.G., 1983. Historical valley alluviation in mid-Wales. Geol. J. 18, 331–350.

Lisle, T.E., 2008. The evolution of sediment waves influenced by varying transport capacity in heterogeneous rivers. In: Habersack, H., Piegay, H., Rinaldi, M. (Eds.), Gravel-Bed Rivers VI: From Process Understanding to River Restoration, pp. 443–469 http://dx.doi.org/10.1016/S0928-2025(07)11136-6.

Lisle, T.E., Cui, Y., Parker, G., Pizzuto, J.E., Dodd, A.M., 2001. The dominance of dispersion in the evaluation of bed material waves in gravel-bed rivers. Earth Surf. Process. Landforms 26, 1409–1420.

Lisle, T.E., Pizzuto, J.E., Ikeda, H., Iseya, F., Kodama, Y., 1997. Evolution of a sediment wave in an experimental channel. Water Resour. Res. 33, 1971. http://dx.doi.org/10.1029/97WR01180.

Macklin, M.G., Lewin, J., 1989. Sediment transfer and transformation of an alluvial valley floor: The River South Tyne, Northumbria, U.K. Earth Surf. Process. Landforms 14, 233–246. http://dx.doi.org/10.1002/esp.3290140305.

Madej, M.A., Ozaki, V., 1996. Channel response to sediment wave propagation and movement, Redwood Creek, California, USA. Earth Surf. Process. Landforms 21, 911–927. http://dx.doi.org/10.1002/(SICI)1096-9837(199610)21:10%3C911::AID-ESP621%3E3.0.CO;2-1.

Magilligan, F.J., 1985. Historical floodplain sedimentation in the Galena River Basin, Wisconsin and Illinois. Ann. Assoc. Am. Geogr. 75, 583–594.

Major, J., Podolak, C.J., Keith, M.K., Grant, G.E., Spicer, K.R., Pittman, S., Bragg, H.M., Wallick, J.R., Tanner, D.Q., Rhode, A., Wilcock, P.R., 2012. Geomorphic response of the Sandy River, Oregon, to removal of Marmot Dam. U.S. Geol. Surv. Prof. Pap. 1792, 64.

McKay, L., Bondelid, T., Dewald, T., Johnston, C., Moore, R., Rea, A., 2012. NHDPlus Version2: User Guide. U.S. Environ. Prot. Agency, Washington, D.C. (URL http://ftp.horizon-systems.com/NHDPlus/NHDPlusV21/Documentation/NHDPlusV2_User_Guide.pdf (accessed 5.20.14)).

Meade, R.H., 1985. Wavelike movement of bedload sediment, East Fork River, Wyoming. Environ. Geol. Water Sci. 7, 215–225. http://dx.doi.org/10.1007/BF02509922.

Nelson, P.A., Brew, A.K., Morgan, J.A., 2015. Morphodynamic response of a variable-width channel to changes in sediment supply. Water Resour. Res. http://dx.doi.org/10.1002/2014WR016806.

Nicholas, A.P., Ashworth, P.J., Kirkby, M.J., Macklin, M.G., Murray, T., 1995. Sediment slugs: large-scale fluctuations in fluvial sediment transport rates and storage volumes. Prog. Phys. Geogr. 19, 500–519. http://dx.doi.org/10.1177/030913339501900404.

Pearce, A.J., Watson, A.J., 1986. Effects of earthquake-induced landslides on sediment budget and transport over a 50-yr period. Geology 14, 52–55.

Pickup, G., Higgins, R.J., Grant, I., 1983. Modelling sediment transport as a moving wave -- the transfer and deposition of mining waste. J. Hydrol. 60, 281–301.

Reid, L.M., Dunne, T., 1984. Sediment production from forest road surfaces. Water Resour. Res. 20, 1753–1761.

Reid, I., Frostick, L.E., Layman, J.T., 1985. The incidence and nature of bedload transport during flood flows in coarse-grained alluvial channels. Earth Surf. Process. Landforms 10, 33–44. http://dx.doi.org/10.1002/esp.3290100107.

Rice, S., 1998. Which tributaries disrupt downstream fining along gravel-bed rivers? Geomorphology 22, 39–56. http://dx.doi.org/10.1016/S0169-555X(97)00052-4.

Saucier, R.T., 1983. Historic changes in Current River meander regime. Proceedings of the Conference, Rivers '83. ASCE, pp. 180–190.

Schottler, S.P., Ulrich, J., Belmont, P., Moore, R., Lauer, J.W., Engstrom, D.R., Almendinger, J.E., 2013. Twentieth century agricultural drainage creates more erosive rivers. Hydrol. Process. 11. http://dx.doi.org/10.1002/hyp.9738.

Sklar, L.S., Fadde, J., Venditti, J.G., Nelson, P., Aleksandra Wydzga, M., Cui, Y., Dietrich, W.E., 2009. Translation and dispersion of sediment pulses in flume experiments simulating gravel augmentation below dams. Water Resour. Res. 45, 1–14. http://dx.doi.org/10.1029/2008WR007346.

Sutherland, D.G., Ball, M.H., Hilton, S.J., Lisle, T.E., 2002. Evolution of a landslide-induced sediment wave in the Navarro River, California. Bull. Geol. Soc. Am. 114, 1036–1048. http://dx.doi.org/10.1130/0016-7606(2002)114<1036:EOALIS>2.0.CO;2.

Trimble, S.W., 1981. Changes in sediment storage in the Coon Creek basin, Driftless area, Wisconsin, 1853 to 1975. Science 214, 181–183. http://dx.doi.org/10.1126/science.214.4517.181.

Trimble, S.W., 1983. A sediment budget for Coon Creek basin in the driftless area, Wisconsin, 1853–1977. Am. J. Sci. 283, 454–474.

Trimble, S.W., 1994. Erosional effects of cattle on streambanks in Tennessee, U.S.A. Earth Surf. Process. Landforms 19, 451–464. http://dx.doi.org/10.1002/esp.3290190506.

Tullos, D., Wang, H.W., 2014. Morphological responses and sediment processes following a typhoon-induced dam failure, Dahan River, Taiwan. Earth Surf. Process. Landforms 39, 245–258. http://dx.doi.org/10.1002/esp.3446.

Venditti, J.G., Dietrich, W.E., Nelson, P.A., Wydzga, M.A., Fadde, J., Sklar, L., 2010a. Effect of sediment pulse grain size on sediment transport rates and bed mobility in gravel bed rivers. J. Geophys. Res. Earth Surf. 115, 1–19. http://dx.doi.org/10.1029/2009JF001418.

Venditti, J.G., Dietrich, W.E., Nelson, P.A., Wydzga, M.A., Fadde, J., Sklar, L., 2010b. Mobilization of coarse surface layers in gravel-bedded rivers by finer gravel bed load. Water Resour. Res. 46, 1–10. http://dx.doi.org/10.1029/2009WR008329.

Wilcox, A.C., Connor, J.E.O., Major, J.J., 2014. Rapid reservoir erosion, hyperconcentrated flow, and downstream deposition triggered by breaching of 38 m tall Condit Dam, White Salmon River, Washington. J. Geophys. Res. Earth Surf. 119, 1376–1394. http://dx.doi.org/10.1002/2013JF003073.

Wohl, E.E., Cenderelli, D.A., 2000. Sediment deposition and transport patterns following a reservoir sediment release. Water Resour. Res. 36, 319–333.

Wu, W., Wang, S., 2006. Formulas for sediment porosity and settling velocity. J. Hydraul. Eng. 132 (8), 858–862.